

Communication

## A Dynamic Three-Dimensional Covalent Organic Framework

Yun-Xiang Ma, Zhi-Jun Li, Lei Wei, San-Yuan Ding, Yue-Biao Zhang, and Wei Wang

*J. Am. Chem. Soc.*, **Just Accepted Manuscript** • DOI: 10.1021/jacs.7b01097 • Publication Date (Web): 28 Mar 2017

Downloaded from <http://pubs.acs.org> on March 28, 2017

### Just Accepted

“Just Accepted” manuscripts have been peer-reviewed and accepted for publication. They are posted online prior to technical editing, formatting for publication and author proofing. The American Chemical Society provides “Just Accepted” as a free service to the research community to expedite the dissemination of scientific material as soon as possible after acceptance. “Just Accepted” manuscripts appear in full in PDF format accompanied by an HTML abstract. “Just Accepted” manuscripts have been fully peer reviewed, but should not be considered the official version of record. They are accessible to all readers and citable by the Digital Object Identifier (DOI®). “Just Accepted” is an optional service offered to authors. Therefore, the “Just Accepted” Web site may not include all articles that will be published in the journal. After a manuscript is technically edited and formatted, it will be removed from the “Just Accepted” Web site and published as an ASAP article. Note that technical editing may introduce minor changes to the manuscript text and/or graphics which could affect content, and all legal disclaimers and ethical guidelines that apply to the journal pertain. ACS cannot be held responsible for errors or consequences arising from the use of information contained in these “Just Accepted” manuscripts.

# A Dynamic Three-Dimensional Covalent Organic Framework

Yun-Xiang Ma,<sup>†,#</sup> Zhi-Jun Li,<sup>†,#</sup> Lei Wei,<sup>‡</sup> San-Yuan Ding,<sup>†</sup> Yue-Biao Zhang,<sup>\*,‡,□</sup> and Wei Wang<sup>\*,†,§</sup>

<sup>†</sup>State Key Laboratory of Applied Organic Chemistry, College of Chemistry and Chemical Engineering, Lanzhou University, Lanzhou, Gansu 730000, China

<sup>\*</sup>School of Physical Science and Technology, ShanghaiTech University, Shanghai 201210, China

<sup>§</sup>Collaborative Innovation Center of Chemical Science and Engineering, Tianjin 300071, China

<sup>□</sup>Joint Laboratory of Low-Carbon Energy Science, Shanghai Advanced Research Institute, Chinese Academy of Sciences, Shanghai 201203, China.

*Supporting Information Placeholder*

**ABSTRACT:** A guest-induced reversible crystal-structure transformation is identified in a new 3D covalent organic framework (COF) by the comprehensive analyses of powder X-ray diffraction, organic vapor sorption isotherm, and <sup>129</sup>Xe NMR spectroscopy. The utilization of revolving imine-bond in interpenetrating 3D networks is uncovered as the key to the dynamic behavior, whose potential applications have been illustrated by gas separation and heterogeneity catalysis, thus, paving the way to the design of stimuli-responsive and multifunctional COF materials.

Dynamic behavior, as evidenced by crystal structure transformation, can be induced in crystalline porous materials by guest molecules, pressure, and temperature. This highly desired property is most often exemplified by metal-organic frameworks (MOFs)<sup>1</sup> in order to achieve stimuli-driven responses for sensing, selective adsorption and separation, gas storage, and heterogeneous catalysis.<sup>2,3</sup> More robust crystalline porous materials, termed covalent organic frameworks (COFs),<sup>4</sup> have emerged as the new frontier for materials, in which the notion that “chemistry of the framework” has been achieved by extending Lewis’ concept of “the atom the molecule” to precisely control and manipulate the structure and function of matter.<sup>5</sup> Great efforts have been devoted to the crystallization and structural determination of COFs, constructed solely by organic building blocks linked entirely through strong covalent bonds into 2D and 3D networks.<sup>6</sup> With a higher degree of flexibility of the constituents, there have been some hints for dynamic behavior in COFs,<sup>7,8</sup> however, principle for the design of dynamic COFs remains largely untapped. Thus, structural elucidation and fundamental understandings are solely needed to propel the exploitation of COFs as stimuli-responsive materials.

Herein, we report the synthesis and characterization of a new 3D COF, termed LZU-301 (LZU = Lanzhou University), synthesized *via* the imine condensation of (3,3'-bipyridine)-6,6'-dicarbaldehyde (BPyDA) and tetra-(4-anilyl)methane (TAM) to give pyridyl-functionalized 1D channels encompassed by the highly interpenetrated diamond networks (**dia-C9-net**, Figure 1). Notably, reversible crystal-transformation and dynamic response of COF have been comprehensively proven by powder X-ray diffraction (PXRD) analysis, organic vapor sorption isotherms, and <sup>129</sup>Xe NMR spectroscopy. We have uncovered that imine bonds revolving as molecular pedal within inter-

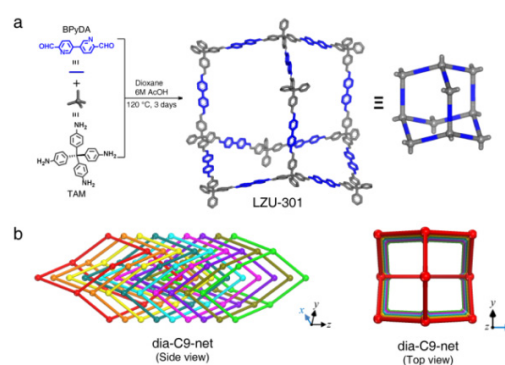


**Figure 1.** (a) Solvothermal synthesis of a three-dimensional (3D) COF material, LZU-301, via imine condensation. For clarity, only the single framework of LZU-301 is shown. (b) Side and top views of porous crystalline structure of LZU-301, which features with a 9-fold interpenetration of the underlying diamond net.

penetrating 3D networks is the key to access such dynamic behavior. LZU-301 is a proven dynamic adsorbent for the selective capture of CO<sub>2</sub> from both dry and humid gas mixtures, in which a water-assisted gating CO<sub>2</sub> adsorption enhancement was observed. Probed by the well-studied Knoevenagel condensation, LZU-301 has shown catalytic activity within pores, capable for the inclusion of large molecules, interaction with substrates, and extrusion of products, showing the possibility for design more advance COF catalysts integrated with dynamic response in the future.

Details of the synthetic procedure and characterization of LZU-301 are provided in the Supporting Information (SI, section S1). The successful formation of the imine linkage was confirmed by both FT-IR (Figures S1–S2) and <sup>13</sup>C solid-state NMR spectroscopy (Figure S3–S5). The crystallinity and phase purity were validated by PXRD (Figures S10–S12) and scanning electron microscopy (SEM, Figure S8). The thermal stability up to 512 °C was indicated by thermogravimetric analysis (TGA, Figure S9). The permanent porosity, specific surface area, and pore volume were assessed by the N<sub>2</sub> physisorption isotherm at 77 K (Figures S21–S23), which show that LZU-301 exhibits microporosity with the Brauner-Emmett-Teller (BET) surface area of 654 m<sup>2</sup> g<sup>-1</sup>. These structural details undoubtedly support the formation of LZU-301 with structural regularity, architectural robustness, and intrinsic porosity.

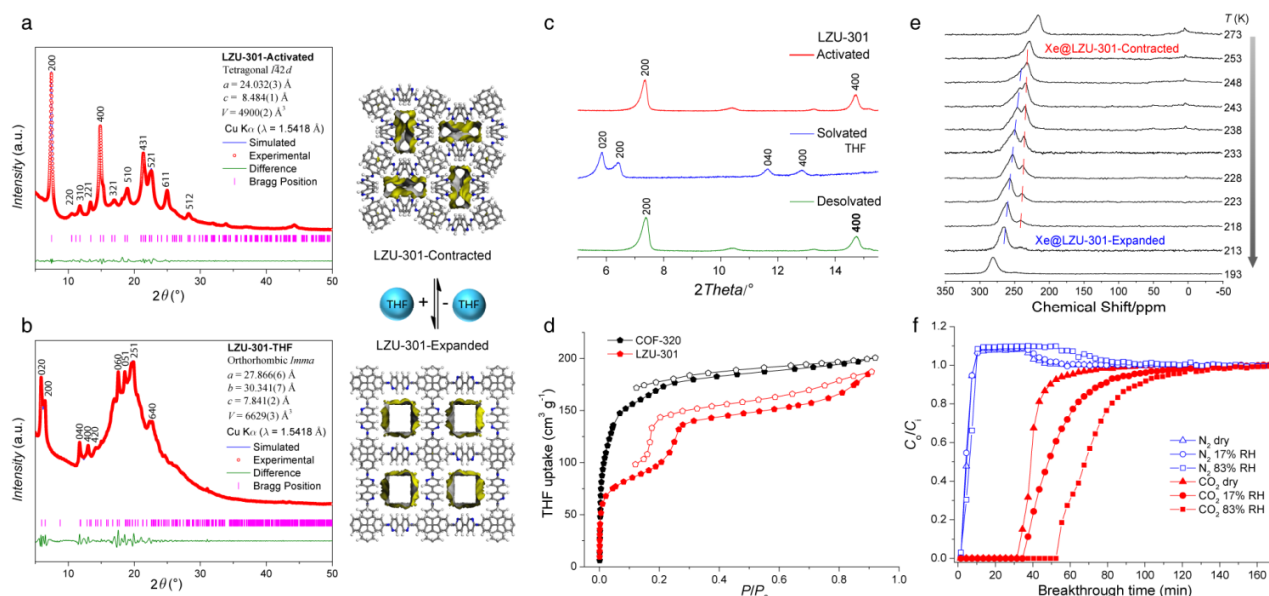


**Figure 2.** (a) Indexed PXRD pattern (red) of activated sample and Pawley fitting profile (blue) supporting the contracted structure (right attached) presents in LZU-301 upon activation. (b) Indexed PXRD pattern of the THF-solvated sample (red) and Pawley fitting profile (blue) supporting the transformation into expanded structure (right attached) upon guest inclusion in LZU-301. (c) Recovery of PXRD patterns upon solvated and desolvated process showing the reversibility of crystal structural transformation. (d) THF vapor adsorption isotherms of LZU-301 and COF-320 at 283 K showing dynamic response to vapor pressure for LZU-301. (e) Temperature-dependent (decreased from 273 to 193 K, initial pressure  $\sim 14.8$  bar)  $^{129}\text{Xe}$  NMR spectra with signals attributed to xenon adsorbed in contracted phase (red line) and expanded phase (blue line) of LZU-301. (f) Breakthrough curves for gas separation of  $\text{CO}_2/\text{N}_2$  ( $v/v = 10:90$ ) under dry and wet conditions (relative humidity, RH = 17% and 83%, respectively) showing the water-induced gating  $\text{CO}_2$  uptake.

The structural elucidation of LZU-301 was based on the reticular chemistry of interpenetration of **dia-net**<sup>7</sup> and single crystal structures of COF-320<sup>8</sup>. By modeling crystal structures with multiple interpenetrations and various symmetries, one of the candidate models (Table S2, space group:  $I\bar{4}2d$ ) with simulated PXRD matched with that of the activated sample, which was amended from the low-temperature phase of COF-320<sup>8</sup> by replacing the benzene ring into pyridyl group and optimizing unit cell with energy minimal. Using this model, the Pawley refinement of the PXRD patterns converged in small differences between the experimental and the simulated profiles (Figure 2a), resulting in unit cell parameters of  $a = b = 24.032(3)$  Å,  $c = 8.484(1)$  Å, and  $V = 4900(2)$  Å<sup>3</sup> (with  $R_{\text{wp}} = 1.81\%$  and  $R_p = 1.35\%$ ; Figure 2a).

The crystal-structure transformation was first observed when a discrepancy was identified between the experimental PXRD patterns of activated and solvated samples of LZU-301 immersed in tetrahydrofuran (THF, Figures 2b and S11), which can be recovered after reactivation (Figures 2c and S11). Similar changes and recoveries of PXRD patterns were also observed for the activated sample solvated with ethanol, acetone, and acetonitrile, where the original 200 peaks split into two peaks and shifts to lower  $2\theta$  angles upon solvation (Figures S13–S16). Comparison of the PXRD patterns of activated and solvated samples demonstrates that a symmetry breaking and lattice expansion were happening.<sup>9</sup> In light of the orthorhombic phase of COF-320<sup>8</sup>, a lower-symmetry model (Table S3) with a space group of *Imma* adapting the unaltered **dia-C9-net** interpenetrated along the  $c$ -axis was built, which is coherent with the observed PXRD pattern. Based on this model, the Pawley refinement provided a perfect fit between the simulated and experimental PXRD profiles ( $R_{\text{wp}} = 1.85\%$  and  $R_p = 1.28\%$ ; Figure 2b). Accordingly, the unit cell parameters increased

to  $a = 27.866(6)$ ,  $b = 30.341(7)$ ,  $c = 7.841(2)$  Å, and  $V = 6629(4)$  Å<sup>3</sup>. Noted is the fact that an exceptional expansion of unit cell volume after solvation is observed (up to 35%), which is attributed to the conformation change of the  $-\text{C}=\text{N}-$  (Figure S17) featuring the ‘pedal’ motion in crystal.<sup>10</sup> The 3D nature in LZU-301 leads to the looser inter-framework packing (7.8–8.5 Å of translation along the  $c$  axis between sets; 3.4–4.8 Å separation between closest layers in comparison with 2D COFs usually having layer separation of 3.3 Å) enabling the revolving of imine bonds.

With the dynamic framework having pore size stretchable from  $5.8 \times 10.4$  Å<sup>2</sup> (contracted form) to  $9.6 \times 10.4$  Å<sup>2</sup> (expanded form), we were puzzled with the one-step shape and lower uptake observed in the  $\text{N}_2$  adsorption isotherm at 77 K with  $P/P_0 = 10^{-5} \sim 0.993$ . Thus, we have recollected the  $\text{N}_2$  adsorption at 77 K with  $P/P_0$  from  $10^{-7}$  to 0.999, which have shown a significant hysteresis of desorption branch (Figure S24), indicating a partially gate opening triggered by the liquid-like  $\text{N}_2$ . Assessed from the adsorption and desorption branches, the surface areas of these two status are 654 and 848 m<sup>2</sup>/g, and pore volumes are 0.3096 and 0.3872 cm<sup>3</sup>/g, respectively. To further visualize the gate-opening effect in LZU-301, vapor adsorption isotherms were collected on both LZU-301 and COF-320 at 283 K (Figure 2d). Significant stepwise and hysteresis uptake was observed from LZU-301 in contrast with the knee shape isotherm for COF-320, indicating LZU-301 retains its contracted phase for dynamic response at higher temperatures but not the case for COF-320. The uptake of the first step reached 81.6 cm<sup>3</sup> g<sup>-1</sup> at  $P/P_0 = 0.08$  with the calculated pore volume 0.295 cm<sup>3</sup> g<sup>-1</sup> and then it reached 167 cm<sup>3</sup> g<sup>-1</sup> at  $P/P_0 = 0.8$  with the calculated pore volume 0.605 cm<sup>3</sup> g<sup>-1</sup> after the second step, corresponding to the theoretical value from the structures of activated LZU-301 (0.296 cm<sup>3</sup> g<sup>-1</sup>) and THF-solvated LZU-301 (0.612 cm<sup>3</sup> g<sup>-1</sup>), respectively.

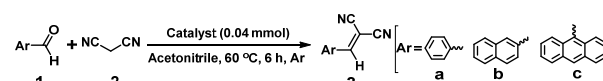
By virtue of the high molecular polarizability and environmentally sensitive NMR signal for xenon guests,<sup>11</sup> the <sup>129</sup>Xe NMR spectroscopy was employed to directly probe the dynamic behavior of LZU-301, which represents the first time this technique has been used for characterizing COF materials.<sup>12</sup> The <sup>129</sup>Xe signals were monitored by cooling down from 273 to 193 K a constant amount of xenon gas within a sealed tube containing LZU-301 (see SI for experimental details). A gradual switch from high field to low field was observed with intermediate states having two split peaks for the <sup>129</sup>Xe signals from 243 to 213 K (Figure 2e). Given the kinetic diameter of xenon (4.4 Å), the contracted LZU-301 (aperture diameters = 5.8 × 10.4 Å<sup>2</sup>) can only accommodate discrete xenon molecules, while the expanded state (aperture diameters = 9.6 × 10.4 Å<sup>2</sup>) provides more space for xenon molecules to closely compact for stronger Xe–Xe interactions,<sup>11b</sup> thus resulting in <sup>129</sup>Xe NMR signals in lower fields. Similar phenomena have been observed for flexible MOFs.<sup>12a</sup> A reversible process was further observed by warming up the sample from 193 to 273 K (Figure S19), in which the <sup>129</sup>Xe signals switched gradually from low to high field. Furthermore, pressure dependent <sup>129</sup>Xe NMR spectroscopy was also performed at 233 K (Figure S20), in which the gradual switch from high to low field was also observed with increasing pressure. All of these results indicate the reversible pore expansion/contraction in the dynamic LZU-301 as stimuli responses to adsorption/desorption.

To exploit the pyridyl moieties in the channel as functional groups for gas separation, CO<sub>2</sub> adsorption properties were assessed by both static adsorption isotherms and dynamic breakthrough curves. Only physisorption was observed in CO<sub>2</sub> adsorption isotherm measured at 273 and 298 K (Figure S27), with uptakes reaching 2.63 and 1.59 mmol g<sup>-1</sup> at 1 bar, respectively. These CO<sub>2</sub> uptake capacities are higher than COFs functionalized with hydroxyl groups and comparable to COFs functionalized with carboxylate or primary alcohol groups.<sup>13</sup> In order to test LZU-301 under practical applications, breakthrough experiments using CO<sub>2</sub>/N<sub>2</sub> gas mixtures *s*(*v/v* = 10:90 at 298 K and 1 bar) under dry or humid conditions were employed<sup>14</sup> (Figure 2f). Sufficiently long retention time of 25 min were observed, in which 0.22 mmol g<sup>-1</sup> of CO<sub>2</sub> was captured under dry conditions, while longer retention times were seen under wet condition [17% relative humidity (RH)]. For the latter, LZU-301 adsorbed 0.29 mmol g<sup>-1</sup> of CO<sub>2</sub>. Interestingly, the CO<sub>2</sub> capture amount was further enhanced to 0.37 mmol/g under 83% RH, which is even higher than the CO<sub>2</sub> uptake (0.35 mmol/g) of the activated framework at 298 K and *P/P*<sub>0</sub> = 0.1, indicating a gate-open effect with the presence of water.<sup>15</sup> Neither decomposition nor chemical adsorption was suggested as evidenced by the solid state <sup>13</sup>C NMR spectrum of LZU-301 after CO<sub>2</sub> sorption under humid condition (Figure S6).

To illustrate the inclusion of large molecules, access of interior functionalities, and potential applications of heterogeneous catalysis, Knoevenagel condensation reactions, previously well-performed by the rigid imine COFs,<sup>16</sup> were tested on the dynamic LZU-301 with the additional pyridyl groups functioning as Lewis base. To trigger the channel expansion of activated LZU-301 as catalyst, the catalytic reactions were conducted in acetonitrile with aromatic aldehydes (**1**) as size probes and malononitrile (**2**) as active methylene reagent to make larger-sized  $\alpha,\beta$ -unsaturated products (**3**). Indeed, catalytic activity of LZU-301 was observed for benzaldehyde (**1a**, 6.5 × 8.5 Å<sup>2</sup>) converted into benzylidene-malononitrile (**3a**, 8.0 × 11.3 Å<sup>2</sup>) with 72% yield in 6 hours outperforming COF-320 (42% yield) and non-porous analogue LZU-101 (21%, see SI for synthesis), and achieved 99% yield in 10 hours. For larger-sized substrates, 2-naphthaldehyde (**1b**, 7.2 × 10.3 Å<sup>2</sup>) and 9-anthraldehyde (**1c**, 8.6 × 11.5 Å<sup>2</sup>), lower activities and yields

were observed, due to the oversized products (**3b**, 12.8 × 8.2 Å<sup>2</sup>; **3c**, 11.4 × 11.5 Å<sup>2</sup>, respectively). To confirm the inclusion of **1c** with size closed to the expanded channel (9.6 × 10.4 Å<sup>2</sup>) of LZU-301, secondary size selectivity<sup>17</sup> was observed by mixed the **1a** and **3a** in the catalytic reaction, where the clogging of **3a** reduced the conversion of **1a**. Control experiments for blank, leaching out, homogeneous catalyst, and non-porous analogue, as well as cycling reaction of LZU-301 were also performed to ensure the reaction is occurred in the channels of LZU-301 (Table 1 and Section S10 in SI).

**Table 1. Knoevenagel condensation catalytic experiments.<sup>a</sup>**



Aldehyde	Product	Isolated yield for different catalysts (%)			
		LZU-301	LZU-101	PyMA <sup>b</sup>	COF-320
<b>1a</b>	<b>3a</b>	72 (99 <sup>c</sup> )	21	94	42
<b>1b</b>	<b>3b</b>	21	22	95	N/A
<b>1c</b>	<b>3c</b>	5	13	75	N/A
<b>1a+1c<sup>d</sup></b>	<b>3a</b>	~18 <sup>e</sup>	N/A	N/A	N/A

<sup>a</sup>General conditions: aldehyde (**1**, 0.5 mmol), malononitrile (**2**, 1.5 mmol). <sup>b</sup>Reaction time: 4 hours. <sup>c</sup>Prolong the reaction time to 10 hours. <sup>d</sup>Ratio of 0.25 mmol vs. 0.25 mmol. <sup>e</sup>GC yield.

As a summary, we have identified the structural transformation and dynamic behavior of a new 3D COF comprehensively via PXRD, vapor adsorption isotherms, and <sup>129</sup>Xe NMR spectroscopy. Beyond the widely used hinge motion of COO–M in breathing MOFs, we disclosed here the –C=N– can serve as a versatile molecular pedal for the design of dynamic COFs. LZU-301 is a proven dynamic adsorbent for the selective capture of CO<sub>2</sub> from both dry and humid gas mixtures, where a water-assisted gating effect for CO<sub>2</sub> capture has been observed for the first time in COF materials.

## ASSOCIATED CONTENT

### Supporting Information

Detailed synthetic procedures, FT-IR spectra, solid-state <sup>13</sup>C CP/MAS NMR spectra, SEM images, PXRD patterns, TGA trace, structure modeling and atom coordinates, gas/vapor sorption isotherms, <sup>129</sup>Xe NMR spectra, and catalytic experiments. These materials are available free of charge via the Internet at <http://pubs.acs.org>.

## AUTHOR INFORMATION

### Corresponding Author

\*zhangyb@shanghaitech.edu.cn;

\*wang\_wei@lzu.edu.cn

### Author Contributions

<sup>#</sup>These authors contributed equally to this work.

### Notes

The authors declare no competing financial interests.

## ACKNOWLEDGMENTS

This work was financially supported by the National Natural Science Foundation of China (No. 21425206 and 21522105). Y.-B.Z. acknowledges the support of the 1000 Young Talent Plan. The authors

thank Dr. P.-Q. Liao and Prof. J.-P. Zhang (Sun Yat-Sen University) for beneficial discussion.

## REFERENCES

- (1) (a) Horike, S.; Shimomura, S.; Kitagawa, S. *Nat. Chem.* **2009**, *1*, 695. (b) Férey, G.; Serre, C. *Chem. Soc. Rev.* **2009**, *38*, 1380. (c) Schneemann, A.; Bon, V.; Schwedler, I.; Senkovska, I.; Kaskel, S.; Fischer, R. A. *Chem. Soc. Rev.* **2014**, *43*, 6062. (d) Zhang, J.-P.; Liao, P.-Q.; Zhou, H.-L.; Lin, R.-B.; Chen, X.-M. *Chem. Soc. Rev.* **2014**, *43*, 5789.
- (2) (a) Rabone, J.; Yue, Y.-F.; Chong, S. Y.; Stylianou, K. C.; Bacsá, J.; Bradshaw, D.; Darling, G. R.; Berry, N. G.; Khimyak, Y. Z.; Ganin, A. Y.; Wiper, P.; Claridge, J. B.; Rosseinsky, M. J. *Science* **2010**, *329*, 1053. (b) Chen, Q.; Chang, Z.; Song, W.-C.; Song, H.; Song, H.-B.; Hu, T.-L.; Bu, X.-H. *Angew. Chem. Int. Ed.* **2013**, *52*, 11550. (c) Mason, J. A.; Oktawiec, J.; Taylor, M. K.; Hudson, M. R.; Rodriguez, J.; Bachman, J. E.; Gonzalez, M. I.; Cervellino, A.; Guagliardi, A.; Brown, C. M.; Llewellyn, P. L.; Masciocchi, N.; Long, J. R. *Nature* **2015**, *527*, 357. (d) Deria, P.; Gómez-Gualdrón, D. A.; Bury, W.; Schaefer, H. T.; Wang, T. C.; Thallapally, P. K.; Sarjeant, A. A.; Snurr, R. Q.; Hupp, J. T.; Farha, O. K. *J. Am. Chem. Soc.* **2015**, *137*, 13183. (e) Krause, S.; Bon, V.; Senkovska, I.; Stoeck, U.; Wallacher, D.; Töbrens, D. M.; Zander, S.; Pillai, R. S.; Maurin, G.; Coudert, F.-X.; Kaskel, S. *Nature* **2016**, *532*, 348.
- (3) (a) Kawamichi, T.; Haneda, T.; Kawano, M.; Fujita, M. *Nature* **2009**, *461*, 633. (b) Das, R. K.; Aijaz, A.; Sharma, M. K.; Lama, P.; Bharadwaj, P. K. *Chem.-Eur. J.* **2012**, *18*, 6866.
- (4) (a) Feng, X.; Ding, X.; Jiang, D. *Chem. Soc. Rev.* **2012**, *41*, 6010. (b) Ding, S.-Y.; Wang, W. *Chem. Soc. Rev.* **2013**, *42*, 548. (c) Colson, J. W.; Dichtel, W. R. *Nat. Chem.* **2013**, *5*, 453. (d) Segura, J. L.; Mancheño, M. J.; Zamora, F. *Chem. Soc. Rev.* **2016**, *45*, 5635.
- (5) (a) Diercks, C.; Yaghi, O. M. *Science* **2017**, *355*, 923. (b) Liu, Y.; Ma, Y.; Zhao, Y.; Sun, X.; Gándara, F.; Furukawa, H.; Liu, Z.; Zhu, H.; Zhu, C.; Suenaga, K.; Oleynikov, P.; Alshammari, A. S.; Zhang, X.; Terasaki, O.; Yaghi, O. M. *Science* **2016**, *351*, 6271.
- (6) Côté, A. P.; Benin, A. I.; Ockwig, N. W.; O'Keeffe, M.; Matzger, A. J.; Yaghi, O. M. *Science* **2005**, *310*, 1166.
- (7) Uribe-Romo, F. J.; Hunt, J. R.; Furukawa, H.; Klöck, C.; O'Keeffe, M.; Yaghi, O. M. *J. Am. Chem. Soc.* **2009**, *131*, 4570.
- (8) Zhang, Y.-B.; Su, J.; Furukawa, H.; Yun, Y.; Gándara, F.; Duong, A.; Zou, X.; Yaghi, O. M. *J. Am. Chem. Soc.* **2013**, *135*, 16336.
- (9) Henke, S.; Schneemann, A.; Wütscher, A.; Fischer, R. A. *J. Am. Chem. Soc.* **2012**, *134*, 9464.
- (10) Harada, J.; Ogawa, K. *Chem. Soc. Rev.* **2009**, *38*, 2244.
- (11) (a) Fraissard, J.; Ito, T. *Zeolites* **1988**, *8*, 350. (b) Bonardet, J.-L.; Fraissard, J.; Gédéon, A.; Springuel-Huet, M.-A. *Catal. Rev.* **1999**, *41*, 115.
- (12) Successful applications in characterizing flexible MOFs: (a) Springuel-Huet, M.-A.; Nossrov, A.; Adem, Z.; Guenneau, F.; Volkringer, C.; Loiseau, T.; Férey, G.; Gédéon, A. *J. Am. Chem. Soc.* **2010**, *132*, 11599. (b) Hoffmann, H. C.; Assfour, B.; Epperlein, F.; Klein, N.; Paasch, S.; Senkovska, I.; Kaskel, S.; Seifert, G.; Brunner, E. *J. Am. Chem. Soc.* **2011**, *133*, 8681.
- (13) (a) Huang, N.; Chen, X.; Krishna, R.; Jiang, D. *Angew. Chem. Int. Ed.* **2015**, *54*, 2986. (b) Huang, N.; Krishna, R.; Jiang, D. *J. Am. Chem. Soc.* **2015**, *137*, 7079.
- (14) Liao, P.-Q.; Chen, H.-Y.; Zhou, D.-D.; Liu, S.-Y.; He, C.-T.; Rui, Z.-B.; Ji, H.-B.; Zhang, J.-P.; Chen, X.-M. *Energy Environ. Sci.* **2015**, *8*, 1011.
- (15) Similar solvent-induced gating CO<sub>2</sub> adsorption has been recently report in MOFs. See: Carrington, E. J.; McAnally, C. A.; Fletcher, A. J.; Thompson, S. P.; Warren, M.; Brammer, L. *Nat. Chem.* **2017**, *ASAP*. DOI: 10.1038/NCHEM.2747.
- (16) (a) Fang, Q.; Gu, S.; Zheng, J.; Zhuang, Z.; Qiu, S.; Yan, Y. *Angew. Chem. Int. Ed.* **2014**, *53*, 2878. (b) Shinde, D. B.; Kandambeth, S.; Pachfule, P.; Kumar, R. R.; Banerjee, R. *Chem. Commun.* **2015**, *51*, 310. (c) Li, H.; Pan, Q.; Ma, Y.; Guan, X.; Xue, M.; Fang, Q.; Yan, Y.; Valtchev, V.; Qiu, S. *J. Am. Chem. Soc.* **2016**, *138*, 14783. (d) Sun, Q.; Aquila, B.; Ma, S.-Q. *Mater. Chem. Front.* **2017**, *ASAP*. DOI: 10.1039/C6QM00363J.
- (17) Khouw, C. B.; Davis, M. E. *ACS Symp. Ser.* **1993**, *517*, 206.

1  
2  
3  
4  
5  
6  
7  
8  
9  
10  
11  
12  
13  
14  
15  
16  
17  
18  
19  
20  
21  
22  
23  
24  
25  
26  
27  
28  
29  
30  
31  
32  
33  
34  
35  
36  
37  
38  
39  
40  
41  
42  
43  
44  
45  
46  
47  
48  
49  
50  
51  
52  
53  
54  
55  
56  
57  
58  
59  
60

TOC

